ELECTROMAGNETIC DESIGN OF RF CAVITIES FOR ACCELERATING LOW-ENERGY MUONS

S.S. Kurennoy, L ANL, Los Alamos, NM 87545, USA

Abstract

A high-gradient linear accelerator for accelerating low-energy muons and pions in a strong solenoidal magnetic field has been proposed for homeland defense and industrial applications [1]. The acceleration starts immediately after collection of pions from a target in a solenoidal magnetic field and brings decay muons, which initially have kinetic energies mostly around 15-20 MeV, to 200 MeV over a distance of ~10 m. At this energy, both ionization cooling and further, more conventional acceleration of the muon beam become feasible. A normal-conducting linac with external-solenoid focusing can provide the required large beam acceptances. The linac consists of independently fed zero-mode (TM_{010}) RF cavities with wide beam apertures closed by thin conducting edge-cooled windows. Electromagnetic design of the cavity, including its RF coupler, tuning and vacuum elements, and field probes, has been developed with the CST MicroWave Studio, and is presented.

INTRODUCTION

Beams of accelerated muons are of great interest for fundamental research as well as for various applications. When a proton beam hits a target pions are produced and decay into muons. Most of the created muons have low energies and are spread in all directions from the target. The 2.2-μs life time of muons is long enough to accelerate them. Muon accelerators are being explored for the Neutrino Factory / Muon Collider (NF/MC) [2] but their huge size and cost prohibit other applications. In the NF/MC projects only a small fraction of all produced muons, those with relatively high energies and traveling in the forward direction, is used. This is justified by the need to have very low emittances for MC but requires a high-power proton driver, which is a $1B-class machine by itself, to provide a sufficient muon flux.

We consider an alternative approach of collecting and accelerating the copious low-energy (tens of MeVs) muons that can lead to smaller and cheaper systems. Accelerated muon beams can enable unique element analysis via muonic X-rays and muon radiography. Compact inexpensive muon accelerators are desired for medical and research applications. These applications have different beam requirements: for muon radiography, a mono-energetic μ^+ beam with minimal divergence is ideal, but μ^- beams for cargo interrogation can benefit from an energy spread and large spot size. In all cases, however, the common task is to accelerate the low-energy muons to higher energies. Therefore, there is a significant interest in a compact and efficient accelerator that can capture a large fraction of a divergent pion-muon distribution from a production target and accelerate muons promptly.

ZERO-MODE CAVITIES

We proposed [1] a novel linac with large acceptance and high gradient that can provide efficient capture and fast acceleration of low-energy muons. Such a linac consists of independently fed zero-mode (TM_{010}) normal-conducting (NC) RF cavities with wide apertures closed by thin metal windows [3]. A guiding axial magnetic field that is created by external super-conducting (SC) solenoids penetrates into the cavities through their metal walls. The linac starts at low beam velocities: around $\beta = v/c = 0.5$ for μ^- produced by a proton beam (the broad peak of muon kinetic energies is 15-20 MeV [4]), or even at $\beta = 0.25$ for μ^+ from a surface muon source (~4 MeV).

Here we present electromagnetic (EM) design of 0-mode cavities for an experimental demonstration of accelerating low-energy muons devised in the framework of the active muon interrogation program. For the demo experiment, it was decided to make an assembly of 4 identical 0-mode RF cavities, and to run the cavities at a reduced gradient, E_0 = 17.5 MV/m, mainly due to the limited peak RF power available, ~5 MW. The high-gradient linac design [1] assumed E_0 = 35 MV/m. The cavity RF frequency is f = 805 MHz. The assembly – RF cavities and their auxiliary elements (couplers, vacuum, cooling, etc) – should fit into a 90-cm bore of the large SC solenoid and operate in the magnetic field up to 5 T. The cavity length $L = \beta\lambda/2$ was chosen to be 10 cm, which corresponds to $\beta = 0.537$, near a broad peak of the muon-velocity distribution at the linac entrance. The cavity layout is illustrated in Fig. 1.

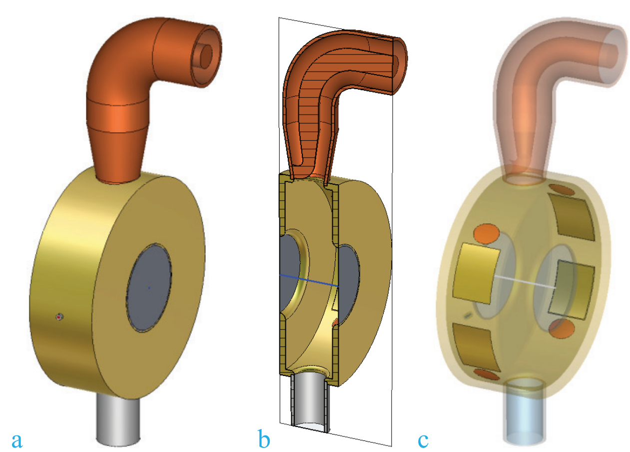

Figure 1: MWS model: (a) cavity (copper) with aperture windows (grey) and RF coupler (brown); (b) cut along the beam axis (blue line); (c) tuning elements highlighted.

The cavity frequency is adjusted by changing its inner radius R. The beam-aperture radius a = 6 cm; the septum full thickness t = 2 cm. The RF coupler is designed to match a rigid 3⅛″ coaxial waveguide. The vacuum pipe is shown in light grey. The cavity aperture edges are blended with radius $t/2$. The demo cavities are designed to be mechanically separate units and can be stacked together with bolts. Neither flanges nor cooling channels in sidewalls and end walls (half-septa) are shown in Fig. 1. A thin edge-cooled aperture window is inserted between two adjacent cavities and clamped to provide good electrical and thermal contact with the common septum formed by two end walls, one from each of two cavities. This allows for easy window replacements when needed. Two end cavities in the assembly have special end cups designed to clamp the aperture window and to create vacuum barrier with a Mylar-film beam window. The mechanical design has been completed but details will not be discussed here. Some dimensions and cavity EM parameters calculated with the CST MicroWave Studio (MWS), both by eigensolver and in time domain, are presented in Table 1 for the gradient E_0 = 17.5 MV/m and duty factor 1%. For power estimates the surface conductivity was reduced by 15% compared to σ = $5.8 \cdot 10^7$ S/m for ideal Cu. The lines in blue are for the cavity with the RF coupler, vacuum and tuning elements.

Table 1: Parameters of the 0-mode cavity in Fig. 1

Parameter (* = at 1% duty)	β_g = 0.537
Cavity inner radius R, cm	14.787
Quality factor Q	19450
Transit-time factor T	0.642
Energy gain eE_0TL, MeV	1.124
Shunt impedance $Z_{sh}T^2$, MΩ/m	17.23
Max electric field E_{max}, MV/m / E_K	22.7 / 0.87
Average surface loss power P, kW*	7.33
Max power flux, W/cm^2* (w/o coupler)	4.5
Aperture surface loss power P_a, %P / W*	2.45 / 180
Coupler aperture radius, cm	2.568
Inner-conductor end radius, cm	1
Inner-conductor-end position h, cm	16.54
External quality factor Q_{ext}	16600
Max power flux, W/cm^2*	14.6
Add. coupler power P_c, % of P / W*	3.0 / 227

Without RF coupler, the total power dissipated on the side wall is 34.6% of the cavity power, while the total power at each end wall is 32.7%; the last figure includes power loss at the window, 1.23 % of the cavity power at each inner window surface. The maximal power density is achieved near the coupler-cavity connection; this is in spite of the fact that the edges of the coupler aperture are rounded with radius 4 mm. Still the total additional power loss due to the coupler is about 3% of the total power deposited in the cavity.

Variations of the cavity dimensions can change its resonance frequency. The strongest dependence is on the cavity radius: df/dR = -5.69 MHz/mm, close to analytical estimate for the TM_{010} mode in a pure pillbox of the same size, -5.45 MHz/mm. Other dependences are weaker: df/dL = -0.31 MHz/mm, where L is the cavity length (would be 0 in the pillbox); and df/dt_w = -2.05 MHz/mm, where t_w is the aperture-window thickness. From these values one can estimate the frequency temperature dependence: the resonance frequency changes by less than 40 kHz when temperature changes by ΔT = 5°F.

Edge-Cooled Thin Aperture Windows

A linac based on isolated cavities with apertures closed by metal windows can work efficiently only for muons, due to their high penetrating ability. The energy loss by low-energy muons passing through the aperture window is an important consideration for the cavity design. Unlike the NF/MC approach, where the forward-produced pions and muons already have significant energies, 100-300 MeV, near the minimal ionization loss ‹-dE/dx›, for low-energy muons the ionization losses are higher, so the windows should be thin to see any acceleration. Monte-Carlo simulations [4] indicate that muons with kinetic energies T_μ = 15-20 MeV loose on average 0.35 MeV in a Be window of 0.5-mm thickness. Taking into account the energy gain per cavity in Table 1 and this energy loss in the windows, the maximal muon energy gain in 4 demo cavities, which contain 5 windows, becomes only about 2.75 MeV. The energy lost in a similar copper window would be a few times higher, completely eliminating any energy gain. This is why we need very thin windows made of low-Z material in the demo cavities. Using a low-Z material also reduces the nuclear scattering.

On the other hand, 2.5% of the RF power in the cavity is deposited on the aperture windows, cf. Table 1. At E_0 = 35 MV/m this power would be in the kW range, even at duty factors of a few percent, so the window cooling is an engineering challenge. Edge-cooled thin-wall windows with cooling channels located in the septum have been explored in [5]. We analyzed a few metal options but finally decided on a thin (0.5 mm) flat carbon window made of graphite coated on both sides with two very thin copper layers (5 µm ≈ 2 skin depths) to carry surface currents. Good thermal properties of graphite and its low expansion coefficient reduce the stresses in the window, which was confirmed by the thermal-stress analysis. The windows were fabricated from Graphtek GM-10 graphite and Cu electroplated. Their thermal and mechanical performance satisfies the cavity requirements, as was proved experimentally using industrial heaters [5]. Testing the RF performance of the windows is one of the goals of the demo experiment.

RF Coupler and Auxiliary Elements

RF power into each of the 4 demo cavities will be fed separately through a 3⅛″ rigid coaxial waveguide connected to the cavity via an RF coupler on the cavity side wall. The coupler must fit into a small length, less than L - t = 10 - 2 = 8 cm, on that wall, plus leave some room for cooling channels and flanges to connect adjacent cavities. Therefore, a tapered transition region is required; it is chosen as a conical transition from 3″- to 2″-coax

 ISBN 978-3-95450-115-1

over the distance of 5 cm. The coupling loop is created by bending the inner conductor and connecting it to the wall of the coax outer conductor; see Fig. 1. The RF coupling is adjusted in MWS simulations by changing the location of this connection. Since the demo cavity has to work inside a solenoid of 90-cm inner diameter, the RF coupler should also provide a 90° bend so that the coaxial waveguide can be connected to it while being directed parallel to the solenoid axis. The coax bend radius was chosen to be 8 cm; this choice places the coupler most outer point at about 40 cm from the cavity (and solenoid) axis and leaves some room for the flanges connecting a straight section of the coaxial waveguide. Combining the above requirements leads to the RF coupler design shown in Fig. 1. The coupling sensitivity was calculated to be $\Delta Q_{ext}/\Delta h \approx 2000$/mm, where h is the distance between the coupler inner-conductor-end center and the beam axis. The cavity is designed to be slightly over-coupled, with the coupling coefficient $\beta_c = Q/Q_{ext} \approx 1.17$. The reflected RF power will be low, below 3% of the input power, in the case of a perfect window-cavity contact; it will still remain below 3% even when the imperfect contact reduces the cavity unloaded Q-factor by any amount in the range from 0% to 27%.

The auxiliary elements of the cavity provide vacuum pumping, rough and fine frequency tuning, and field measuring. While some pumping can be done through the coupler aperture and RF coaxial feed, the main vacuum pipe is connected to the side wall in the location opposite to the coupler, Fig. 1. Its size was chosen the same as for the coupler aperture, but the edge blending radius is made larger, 5 mm vs. 4 mm at the coupler, to reduce surface-current enhancements. Adding the vacuum pipe reduces the cavity resonance frequency by ≈1.5 MHz.

For rough tuning, to be performed before brazing the end plates to the side wall, we insert tuning rings (or rough-tuning patches) on the cavity inner cylindrical wall. The ring width along the cavity axis is 6 cm. When these patches cover 60° of the cavity azimuth, the frequency shift is up by about 3 MHz for the patch thickness (its protrusion into the cavity) equal to 2 mm. This means that in the assembled cavity with the RF coupler, vacuum pipe, and full-height (2 mm) tuning patches, the resonance frequency should be a bit high, ≈1.5 MHz above 805 MHz. The patches can be arranged inside the cavity azimuthally in various ways, as convenient for mechanical design, e.g. 4 pieces as in Fig. 1c. The edges of the tuning patches are blended. Taking off some metal from the tuning rings after frequency measurements in a cold cavity (a stack assembly, not brazed) brings the frequency down. About half of the tuning ring thickness should be removed to bring the resonance frequency to its nominal value, 805 MHz, or a few tens of kHz lower.

For fine tuning of brazed and assembled cavities, fine-tuning patches are incorporated in the design. A fine-tuning patch is an area on the cavity side wall, where the regular wall thickness is noticeably reduced, to ~3 mm of the copper thickness remaining. Such patches can be slightly protruded (dimpled) into the assembled cavity by applying an external force; this should bring the resonance frequency up a bit. While the exact shape of such protrusions is not well defined, we model their effect in the MWS by using shallow spherical segments shown in orange in Fig. 1c. With 4 patches of radius 2 cm, the frequency shift Δf depends on the protrusion depth (segment height along its symmetry axis) d as follows: Δf = 85 kHz for d = 1 mm and Δf = 258 kHz for d = 2 mm. If the number of fine-tuning patches is reduced, the tuning range decreases proportionally to their number.

Measuring the cavity fields is planned with a small coaxial probe that can be seen as a tiny feature on the front-looking cavity side wall in Fig. 1a. It is based on a standard SMA connector: a 50-Ω coax line with its inner conductor of radius 0.25 mm and outer-conductor inner radius of 1.65 mm. The inner conductor is bent 90° and soldered to the outer one at the cavity inner side wall. The line is filled with a dielectric having the electric permittivity $\varepsilon_r = 5.13$. MWS time-domain simulations of the cavity with the field probe give the transmission coefficient from the input RF coax port to the probe port $|S_{21}| = 2.2\cdot10^{-3}$, or – 53.15 dB, at 805 MHz. As a result, the signal power in the field probe is $|S_{21}|^2 = 4.84\cdot10^{-6}$ of the RF input power. For the peak RF input of 758 kW, the probe power is 3.7 W.

To keep open an option of running the demo cavities at higher gradients, a larger RF coupler has been designed for connecting a 4½″ rigid coaxial waveguide, see in [6].

CONCLUSIONS

The electromagnetic design of the zero-mode RF cavities with wide beam apertures closed by thin conducting edge-cooled windows has been developed with the MWS and is presented above. More details can be found in the report [6]. The author would like to acknowledge useful discussions with W.B. Haynes, A.J. Jason, H. Miyadera, W.P. Romero, and W.M. Tuzel.

REFERENCES

[1] S.S. Kurennoy, A.J. Jason, H. Miyadera, "Large-Acceptance Linac for Accelerating Low-Energy Muons," IPAC10, Kyoto, Japan, p. 3518 (2010).
[2] J.S. Berg et al, Phys. Rev. ST-AB, 9, 011001 (2006).
[3] S. Kurennoy, Tech notes AOT-ABS 09-004, -008 (TN), 2009; LA-UR-10-00246, Los Alamos, 2010.
[4] H. Miyadera, A. Jason, S. Kurennoy, "Simulations of a large acceptance linac for muons," PAC09, Vancouver, BC, p. 3555 (2009); H. Miyadera, private communication, 2011.
[5] S.S. Kurennoy, W.M. Tuzel, A.J. Jason, "Aperture Windows in High-Gradient Cavities for Accelerating Low-Energy Muons," IPAC11, San Sebastian, Spain, p. 862 (2011); http://www.JACoW.org
[6] S. Kurennoy, Tech note AOT-ABS 11-020 (TN), 2011; LA-UR-11-11968, Los Alamos, 2011.